Ectomycorrhizal fungi mediate belowground carbon transfer between pines and oaks

Ectomycorrhizal fungi mediate belowground carbon transfer between pines and oaks

Rotem Cahanovitc[1*], Stav Livne-Luzon[1*], Roey Angel[2], Tamir Klein[1*]

[1] Department of Plant & Environmental Sciences, Weizmann Institute of Science, Rehovot 76100, Israel

[2] Soil and Water Research Infrastructure and Institute of Soil Biology, Biology Centre CAS, České Budějovice, Czech Republic

* These authors contributed equally to the study

Corresponding Author: Tamir Klein, tamir.klein@weizmann.ac.il. Tel.: +972-8934-3505

Keywords: common mycorrhizal network; rhizosphere; tree-tree carbon transfer; carbon labeling; stable isotope probing.

Word count: 6501. Introduction, 886; M&M, 2472; Results, 1163; Discussion 1980.

Abstract

Inter-kingdom belowground carbon (C) transfer is a significant, yet hidden, biological phenomenon, due to the complexity and highly dynamic nature of soil ecology. Among key biotic agents influencing C allocation belowground are ectomycorrhizal fungi (EMF). EMF symbiosis can extend beyond the single tree-fungus partnership to form common mycorrhizal networks (CMNs). Despite the high prevalence of CMNs in forests, little is known about the identity of the EMF transferring the C and how these in turn affect the dynamics of C transfer. Here, *Pinus halepensis* and *Quercus calliprinos* saplings growing in forest soil were labeled using a $^{13}CO_2$ labeling system. Repeated samplings were applied during 36 days to trace how ^{13}C was distributed along the tree-fungus-tree pathway. To identify the fungal species active in the transfer, mycorrhizal fine root tips were used for DNA-stable isotope probing (SIP) with $^{13}CO_2$ followed by sequencing of labelled DNA. Assimilated $^{13}CO_2$ reached tree roots within four days and was then transferred to various EMF species. C was transferred across all four tree species combinations. While *Tomentella ellisii* was the primary fungal mediator between pines and oaks, *Terfezia pini*, *Pustularia* spp., and *Tuber oligospermum* controlled C transfer among pines. We demonstrate at a high temporal, quantitative, and taxonomic resolution, that C from EMF host trees moved into EMF and that C was transferred further to neighboring trees of similar and distinct phylogenies.

Introduction

Belowground mutualistic interactions play an essential role in maintaining forest stability around the globe [1]. Ectomycorrhizal fungi (EMF) form extraradical mycelium, a collection of filamentous fungal hyphae emanating from the root, which aid in exploring and exploiting the soil matrix environment [2]. EMF symbiosis is based on the reciprocal exchange of resources [3], and can positively influence the host plant water relations and response to drought [4], and increase its resistance to soil-borne pathogens [5]. Interestingly, EMF symbiosis can extend beyond the single tree-fungus partnership to form common mycorrhizal networks (CMNs) [6]. These networks simultaneously connect multiple plant hosts and mycorrhizal fungi [7], colonizing a large number of plants from the same or different species [8]. For example, CMNs can link hosts belonging to angiosperms and gymnosperms [9], even though these clades diverged during the Jurassic age around 200 M years ago [10]. In addition, CMNs have been found to enhance sapling establishment [11–13], transfer water and reduce water stress [14,15], play a crucial role in C cycling and sequestration [16], and even communicate stress signals among neighboring plants [17].

CMNs have been studied experimentally for many years [18], while their interpretation was continuously criticized [19] and their actual ecological significance for plant fitness has been questioned [20]. Some of the main arguments against these experiments, call for the use of appropriate controls using mesh barriers [21] excluding root-root contact and passive C diffusion through soil. Several studies [22], [23] have shown that C fixed by one plant transferred to the root system, and presumably the hyphae, of the second plant. However, for C to have any eco-physiological importance for the recipient plant, it needs to move out of the roots of the recipient plant. Despite the high prevalence of CMNs in nature, Some of the open questions include the significance of the resources exchange between trees [24], and who are the fungal mediators of the resource exchange [25]. . To better understand CMNs role in ecological communities, various labeling methods have been used [26], and particularly ^{13}C has gained popularity among researchers since C is the primary resource traded among the trees and fungi. Labeling techniques have been tested in both artificial [27–30] and natural systems [13,31,32]. The results from these studies indicate that the bi-directional C transfer between trees can be dictated via a source-sink relationship [31], the amount of overlap in EMF communities between the various hosts [33], and tree phylogenetic relatedness [34]. However, bidirectional transfer was also found between taxonomically distant mature tree taxa (Klein, Siegwolf, and Körner, 2016).

To unravel the importance of C transfer within CMNs and how it relates to the host species' identity and function, we need to identify the EMF involved in the process of C transfer among hosts. Most studies on CMNs have presented indirect or circumstantial evidence while ruling out other alternative mechanisms. At the same time, ^{13}C-DNA-Stable Isotope Probing (SIP) has been used to identify microbial partners in several plant-microbe systems [35–37]. DNA-SIP allows identifying which organisms utilized a substrate of interest using a stable isotope tracer. If an organism incorporates ^{13}C into its nucleotide sugar bases, then the ^{13}C-DNA can be separated from the ^{12}C-DNA using density-gradient centrifugation and sequenced. Despite its potential, ^{13}C-SIP has not yet been applied in the study of C transfer between trees.

In this work, we established a simplified network of a tree-fungi-tree system to directly identify the EMF species serving as the mediators within the CMNs using a ^{13}C labeling approach. Further, we tested if species relatedness is important for plant-plant C transfer. We planted the gymnosperm *Pinus halepensis* (Aleppo Pine) and the angiosperm *Quercus calliprinos* (Palestine oak) in custom-made containers with mesh barriers, allowing CMNs to develop between the trees while prohibiting direct root-root contact. Plant labeling experiments, mostly employ sterile soil and controlled inoculation of one or two EMF species [38]. In contrast, we used natural forest soil, giving the saplings the possibility to form symbiosis with a variety of fungal species. We used saplings of *Pinus* and *Quercus* which belong to the most common tree genera globally, populating vast conifer and broadleaf forests (respectively) across temperate, boreal, and sub-tropical biomes. In the Mediterranean woodland, they colonize similar ecological niches [39,40], and their mixing in forests seems to mutually improve seedling establishment under xeric conditions [41]. Furthermore, they share EMF species [42], raising the possibility for forming CMNs. We used a $^{13}CO_2$ labeling system followed by a high-resolution tissue sampling regime and DNA-SIP to explore (i) whether C transfer occurred; (ii) if so, at which species combinations; (iii) at what temporal and quantitative dynamics; and finally, (iv) which EMFs were involved in C transfer between neighboring trees. We hypothesized that C transfer occurs between neighbouring trees provided that they share EMF species, regardless of their phylogenetic distance, and that EMF are involved in C transfer via the formation of CMNs.

Materials & Methods

Plant and soil material

Soil was collected from the Harel Forest, located ca. 4 km south-west of the town of Beit Shemesh, Israel (31° 43′ N, 34° 57′ E, 320 m elevation). The vegetation comprises local Mediterranean diversity, such as the gymnosperm tree species *Pinus halepensis* and *Cupressus sempervirens*, and local Mediterranean angiosperm woody species, such as *Quercus calliprinos, Ceratonia siliqua,* and *Pistacia lentiscus*, accompanied by a rich understory of annual plants that thrive from winter to spring. The soil was taken from the topsoil layer (0-15 cm) and no farther than 10 m of a *Pinus* or *Quercus* trunk to obtain the native soil mycobiome. To allow proper aeration in the containers, the soil used to transplant the sapling was mixed with 50% sea sand (v/v), and its final texture was: sand 83 ± 1%, silt 9.5 ± 1.5%, clay 7.3 ± 2% (n=3; ARO, Gilat, Israel; see Table S1). *Pinus* and *Quercus* saplings at the age of eight and thirteen months (respectively) were collected from KKL-JNF nursery in Eshtaol, Israel, on 15 December 2019. Following transplantion and immediately prior to labeling the height (cm), diameter (mm), and the number of branches were recorded (Table S2).

Experimental design

The saplings were planted in 10 custom-made containers. Each container (10 cm × 50 cm × 30 cm depth) was divided equally into three compartments, hereafter referred to as 'Control,' 'Donor,' and 'Recipient,' each containing one sapling. "Recipient" and "Control" denote unlabeled plants, and "Donor" denotes a labeled plant. We acknowledge that the movement of nutrients is hypothesized to be bi-directional; the compartment names do not indicate the direction the nutrients move but rather the expected transfer direction of the label. The Control sapling was transplanted with a polycarbonate sheet separating the belowground compartment entirely from the rest of the container. Before inserting soil and saplings into the pots, water was filled in the control compartment and left for 24 h to verify that there were no leaks that would allow a passive transfer between donor and control soil compartments. In the center of the container, the Donor sapling was planted, separated from the Recipient sapling with a 35 µm stainless steel mesh net (Xmd metal mesh, Xinxiang, China), to exclude direct contact of the sapling's roots [21]. The saplings were planted in four species combinations, *Pinus-Pinus-Pinus, Pinus-Quercus-Pinus, Quercus-Quercus-Quercus, Quercus-Pinus-Quercus*, alternating the middle Donor sapling and the adjacent Control and Recipient saplings. Saplings grew together for seven months. Ten containers totaling thirty plants of similar size and phenotype were chosen for the labeling experiment, eight containers (n=24 saplings) which were inserted into the labeling system, and two containers serving as "Unlabeled control", (n=6 saplings).Saplings were kept at full sunlight and were irrigated throughout the experiment. We

irrigated to field capacity at the end of each sampling day, to ensure adequate soil moisture at all times.

Labeling system

A hermetically sealed labeling system explicitly designed for this experiment was built from two parts (Fig. S1). (i) A humidity-controlled glovebox (Coy lab products, Grass Lake, MI, USA) with built-in closed-circuit air condition was used to control and monitor the gas mixture's humidity and temperature, which was introduced to the saplings. To detect $^{13}CO_2$ / $^{12}CO_2$ concentrations, we attached two sensors: PP systems gas analyzer (PP Systems, Amesbury, MA, USA) and G2131-i Picarro cavity ring-down spectrometer (CRDS; Picarro, CA, USA). (ii) A custom-made enclosure was attached to the glovebox built from plexiglass and polyethylene. The enclosure sealed the crowns of eight Donor plants from the surrounding environment. This design included two replicates from each species combination (n=2), totaling 24 saplings. All three belowground compartments of the container and the crowns of adjacent Recipient and Control saplings were excluded from the enclosure. Two fans (24 W Europlast; Drautal, Austria) were used in opposite directions to create air circulation. The humidity and temperature were monitored using three data logger sensors (EasyLog EL-USB-2-LCD, Lascar Electronics, Wiltshire, UK), two on opposite sides of the enclosure box and one in the glovebox. An external air conditioner (R-YDH-5500, Feishi, Shanghai, China) was used to control the temperature.

$^{13}CO_2$ labeling

Eight containers, 24 saplings, two of each species combination, were inserted into the labeling system, where only the middle Donor sapling crown was covered (Fig. S1). The two remaining containers were kept 150 m away from the labeling apparatus and were not labeled, referred to as Unlabeled control, with the *Pinus*-*Pinus*-*Pinus*, *Quercus*-*Quercus*-*Quercus* species combinationsThe labeling started on 13 July 2020 for three consecutive days, starting each day two hours after sunrise, and finishing at sunset, 19:30, totaling 30 hours of labeling. On the first day, 45 grams of sodium bicarbonate 99% ^{13}C dissolved in chloric acid (Sigma, Rehovot, Israel) was used. On the second and third days, we used gaseous $^{13}CO_2$ at equivalent amounts (Sigma, Rehovot, Israel). At the beginning of every labeling day, the CO_2 concentration was lowered to 90.6 ± 24.2 ppm by emptying the headspace using a vacuum pump (Vacuubrand, CT, USA) while simultaneously flushing it with an 80% N^2, 20% O^2 mixture (Maxima, Ashdod, Israel). Light intensity fluctuated around 1,500 µmol m^{-2} s^{-1} throughout the day, (Li-250A light meter, Li-cor, NE, USA). Temperature and relative humidity were kept at 33 ± 3 °C and 65 ± 7% inside the enclosure, respectively. Leaf CO_2 and H_2O

gas exchange measurements were done on mature leaves using a photosynthesis system (IRGA; GFS-3000, Walz, Effeltrich, Germany). The conditions inside the IRGA cuvette were set to a CO_2 level of 400 ppm; flow rate 750 µmol s^{-1}; no temperature or humidity control; and photosynthetically active radiation (PAR) of 1525 ± 75 µmol m^{-2} s^{-1}). To estimate isotopic signals in the soil compartment, a hole was drilled at a depth of 5 cm in each of the three compartments at each of the ten containers, and a hard-plastic tube (2 cm diameter) with holes was inserted. The tube was attached to the CRDS unit, which determined $\delta^{13}C$ respired from the soil compartment. The high sensitivity of CRDS unit inserted into the soil compartments of the three treatments allowed us to verify that no passive transfer occurred due to leakage from the donor compartment. Further details regarding labeling apparatus appear in previous labeling done in our lab [43].

Plant sampling

Plants were sampled and tissues harvested according to the expected amount of label to avoid isotopic contamination during sample handling, from the lowest (i.e., Unlabeled controls) to the highest (i.e., Donor plants). Eleven sampling days, including baseline samples and post-labeling samples, were carried during 36 days. On each day, first-order lateral roots and leaf tissue were taken for analysis from each plant, and on three sampling days stem samples were also collected. Despite the extensive sampling, all samples were negligible in size, about three orders of magnitude smaller than the biomass of the tissue (e.g. 33 mg root tissue sample from a total 10-25 g root biomass, with an even larger shoot biomass of 30-100 g). In addition, sampling was performed with extra care to minimize disturbance to plant and soil, and was uniform across plants. The roots were thoroughly washed on a 1-mm meshed sieve using DDW, and root tips colonized with mycorrhiza (~33 mg each) were separated using sterilized forceps under a binocular and inserted into a 2 ml Eppendorf tube. The tubes were immersed in liquid nitrogen, lyophilized, and stored at -20 °C until DNA extraction. The remaining root (n=326) , leaf (n=297), and stem (n=152) samples were dried for 48 h in a 60 °C oven and then ground for the $\delta^{13}C$ analysis. During each sampling day total soil respiration and $\delta^{13}C$ were measured as explained above.

Plant harvesting and analysis

On 17 August 2020, following the disassembly of the experiment, extensive sampling was carried out to determine the ^{13}C variation in stem, leaf, and root tissues. Each plant was gently separated from the soil and was divided into its components. The soil and roots were thoroughly checked for the existence of mycelial networks (Fig. S2, S3). Five roots were randomly chosen and treated as described above. Stem and leaf samples were taken at two heights, including two leaves representing

mature and young leaves. An additional pooled sample of 30 leaves was ground. Afterward, the remaining biomass was divided to above- and belowground, dried for 48 h in a 60 °C oven, and weighed. Ground tissue samples were weighed to 1.2 g and were measured using a combustion module attached to the Picarro G2131-i unit. After dismantling the experiment and removing the plants and soil, the compartments were examined thoroughly to verify that no leakage occurred due to technical failure of the mesh net or polycarbonate sheet separating the compartments.

DNA extraction

Root tips were collected from four *P. halepensis* Donors and their respective Recipient partners, two *P. halepensis* and two *Q. calliprinos* saplings. Two sampling days were chosen, 9 July 2020 as day 0 and 21 July 2020, 9 days post labeling. Thus, these samples represent the pre-labeling and peak-labeling of the Recipients. Root tips were thawed, and DNA was extracted from them using DNeasy Blood & Tissue Kit (Qiagen, Hilden, Germany) according to the manufacturer's protocol with the following modifications: (1) Pretreatment grinding with a bead beater at 4000 RPM (Restch GmbH, Haan, Germany) for 2 min; (2) Suspension of samples in 700 µl CTAB / PVP buffer and incubation in a water bath (65 °C) for 1 hour; (3) 600 µl chloroform and centrifuged 10 min at 13,000 G. Concentrations of extracted dsDNA were measured fluorometrically using Qubit 2.0 Fluorometer (Thermo Fisher Scientific, Waltham, USA). The DNA extracts were used for stable isotope probing (SIP) density gradient ultracentrifugation (below).

DNA Stable Isotope Probing (DNA-SIP)

For DNA-SIP, we used a published protocol [4422]with the following modifications: 4 ±1.6 µg DNA samples were loaded onto gradient buffer (GB) to a total volume of 1.15 ml. The GB + DNA solution was mixed with 5 mL of cesium chloride (CsCl, Thermo Scientific, Waltham, USA). The solution refractive index was measured (AR200 digital Reichert, Depew, NY, USA) to a target value of 1.4030 ± 0.000. The final solution was loaded onto quick-seal polypropylene centrifuge tubes (Beckman Coulter, Brea, CA, USA). The tubes were sealed and centrifuged for 39 h at 170,000 G at 20 °C (WX model ultracentrifuge Sorvall Thermo Fisher Scientific, Waltham, USA) using an NVT 65.2 rotor (Beckman Coulter). Immediately after centrifugation, 16 fractions containing 350 ± 25 µl each were collected from each gradient, and their refractive index was measured. Next, the DNA was precipitated using PEG solution (Polyethylene glycol 6000, Thermo Scientific;[45] and 2 µl GlycoBlue co-precipitate (Thermo Scientific) and eluted in 30 µl of TE-buffer. In each fraction, DNA concentration was measured with Qubit.

ITS2 region amplification and MiSeq sequencing

Root tip DNA from four Donor pines and the reciprocal Recipient and Control pines and oaks were sequenced to elucidate their fungal community. For this purpose, barcoded amplicon sequencing of the fungal ITS2 region [46] was performed on a MiSeq platform (Illumina, San Diego, CA, USA). From each individual, two sets of root tips harvested on day 0 and day 9 were sampled. From each SIP gradient, 11 out of the 16 fractions (corresponding to densities 1.68-1.77 g ml^{-1}) were sequenced, while the terminal 2-3 fractions from each side were discarded. Two separate sequencing libraries were prepared, the 1st library containing the samples collected from four pine Donors and the 2nd of the corresponding Recipient pairs, two oaks, and two pines. PCR amplification and barcoding was done in a two-step procedure. The first PCR had an initial denaturation at 98°C for 3 min, followed by 32 cycles of 98 °C for 20 s, 50 °C for 30 s and 72 °C for 30 s, and a final extension at 72 °C for 10 min. Each amplification was carried out in a 50 µl reaction mixture containing 25 µl KAPA HiFi ready mix (Eppendorf-5Prime, Gaithersburg, MD, USA), 0.5 µM forward primer, 0.5 µM reverse primer, 5 µl template DNA, and 15 µl nuclease-free water. Fungus specific primers were used, 5.8-Fun and ITS4-Fun (5'-AAC TTT YRR CAA YGG ATC WCT-3', 5' -AGC CTC CGC TTA TTG ATA TGC TTA ART-3', respectively[46]). PCR products were screened for successful amplification using standard gel electrophoresis and quantified using a Qubit dsDNA HS kit (Life Technologies Inc., Gaithersburg, MD, USA). The PCR products were purified using AMPure magnetic beads (Beckman Coulter Inc., Brea, CA, USA), following the manufacturer's instructions. Samples were quality checked for amplicon size using the Agilent 2200 Bioanalyzer (Agilent Technologies, Santa Clara, CA, USA). A second PCR step was done to add an adaptor and barcode at the INCPM (Weizmann Institute, Rehovot, Israel). Libraries were prepared using DNA CHIP-seq protocol as described [47]. Briefly, 20 ng from each sample were used for library generation. Each sample went through a process of adapter ligation and PCR with cleanups in between. At the end of the process, each library was quantified by Qubit and was brought to the same molar concentration, then mixed by taking the same volume for each library. The final pool was diluted and loaded into the MiSeq instrument. Sequencing was done on a MiSeq instrument using a V3 600 cycles kit, allocating 0.22 M reads per sample (paired-end sequencing).

Processing of sequence data

We used R (R Core Team, 2018, version 4.0.3) and the RStudio IDE for bioinformatics and statistical analysis. The sequences were processed using the amplicon sequencing DADA2 package v. 1.7.9 in R [48]. Shortly, raw sequences were demultiplexed, and both adapters and barcodes were removed from the samples. Sequences were quality-filtered and trimmed. We only used sequences

longer than 50 bases with a mean number of expected errors below 2 (maxN = 0, maxEE = c(2,5) minLen = 50 truncQ = 2). Paired-end sequences were merged using the MergePairs function. We then applied a dereplication procedure on each sample independently, using derepFastq function. Finally, all files were combined in one single Fasta file to obtain a single amplicon sequence variant (ASV) data file. We removed singletons (minuniquesize = 2) and de novo chimera sequences using removeBimeraDenovo function against the reference database (UNITE/UCHIME reference datasets v.7.2). Sequences were then clustered, and taxonomic assignment (id = 0.98) was done against the UNITE database. Non-fungal ASVs were removed. To further validate our results, we used Sequencher software (Sequencher 5.4.6, Gene Codes Corp.) to examine if the recipient and donor ASV from the two libraries cluster together, with a minimum match of 97% and a minimum overlap of 100 bp.

Statistical analysis

The analysis of CRDS data, was implemented on the root, leaf, and stem datasets. In cases where the residuals were not normally distributed, we employed a square root-transformation on the original data. We analyzed the data using a split-plot design (using aov function implemented in the car package), where the identity of the pairs of donors (D) and recipients (R), D-Qc | R-Qc, D-Ph | R-Qc, D-Qc | R-Ph, D-Ph | R-Qc, was considered as the between-subject factor. The two containers of each pair (n=2) were considered as the experimental units, while the division within each experimental unit into the various treatments (Control, Donor, Recipient, n=3) was considered as a within plot treatment. The measurement days (n=11) were considered as an additional, random, within-subject factor. The analysis of DNA-SIP data was done with R package Multiple Window High-Resolution Stable Isotope Probing (MW-HR-SIP) as previously described [49], based on the principles of DESeq2. Briefly, four density windows were set: 1.71-1.72, 1.73-1.74, 1.75-1.76, 1.76-1.77, and for each sapling, the unlabeled gradient from day 0 was compared with the matching labeled gradient from day 9. Day 9 was chosen as it was the peak of labeling that appeared in the recipient treatment. If there was a substantial log fold change (after p-value adjustment and correction for multiple comparisons) per the matching fraction at the set density window, it was recorded and manually examined. MW-HR-SIP is based on DESeq2 gene comparison data, uses t-test and corrections for multiple comparisons, and does not test for interaction or include covariates. Further verification of our results was done using the Corncob R package [50]. Corncob is a beta-binomial regression model for microbial taxon abundances, which allows for an association between the variance of a taxon's abundance and covariates.

Results

Labeled C was transferred belowground between trees across four tree combinations

Across the four *Quercus* and *Pinus* combinations and in six out of eight replicates, ^{13}C was found in the Recipient trees' roots and stems but not in their leaves (Fig. 1). When *Pinus* was the Donor, more ^{13}C was found in the Recipient roots than with *Quercus* as a Donor (Fig. S4). On day 0, all saplings' leaves showed natural $\delta^{13}C$ signatures, of -29 - -32‰ (Fig. S4). Following the three-day labeling, leaves in the labeled Donor trees showed values of 5000‰ and beyond (5000‰ being the CRDS upper detection limit), and after 36 days averaged 1850 ± 804‰. Notably, in all but three Recipient replicates, Recipient and Control saplings' leaves did not rise above the $\delta^{13}C$ natural variation. These samples originated from three separate *Pinus* trees on several dates: one sample from day 29 (437‰), the other two from day 5 (18‰ and -2‰). These samples represent three samples which exhibited unexpected values out of the 297 total samples analyzed, and thus was concluded that these outliers were probably the result of human error due to contamination during sample collection and handling, and were removed. The points were handled statistically by replacing their value with the average of the individual sapling the day before and after the removed data point. Comparing all treatments of leaf samples, there was a significant difference ($F_{2,108}$=2844, $p < 0.001$). However, contrasting only the Recipient and Control treatments, we found no significant difference ($F_{1,92}$=0.0001, $p > 0.05$), indicating no labeling of the Recipient leaves.

Labeled C identified in recipient and donor stems and roots but not in control

Substantial amounts of ^{13}C were found in the stems of Donors (Fig. 1; Fig. S5), 2091 ± 1140‰ averaging all measurement days. Among Recipients, labeling was found on day 18, averaging -21 ± 5.6‰ and decreasing subsequently to -25 ± 2‰ on day 36. The control trees maintained a natural $\delta^{13}C$ signature. Comparing all treatments, there was a significant difference ($F_{2,32}$=79, $p < 0.001$) that prevailed when contrasting the recipient and control treatments only ($F_{1,20}$=7.2, $p = 0.015$)**.** Donor $\delta^{13}C$ increased in roots, 3467 ± 1734‰ at day 4, and 1531 ± 571‰ at day 36 (Fig. 2). In the recipient treatment, a gradual increase of $\delta^{13}C$ was observed, peaking at day 9 for both species (7 ± 39‰ in *Quercus*, -7 ± 34.6‰ in *Pinus*). Subsequently, there was a decline of $\delta^{13}C$, with day 36 values still above natural variation (-22 ± 4‰ in *Quercus*, -21 ± 5.3‰ in *Pinus*). Control treatment showed no increase in $\delta^{13}C$, -27 ± 1.4‰ in *Quercus*, -26 ± 2.5‰ in *Pinus* across all measurement days (Table 1). The effects of day and treatment were significant, (Table 1; $F_{10,128}$=3.8, $p < 0.0001$, $F_{2,128}$=246, $p < 0.0001$, respectively). The effect of pair combination was not significant ($F_{3,4}$=0.7, $p = 0.595$). Median tests between Recipient root and corresponding Control roots of the same day found that in 7

out of 10 days (excluding day 0), Recipients and Control trees were significantly different (Table S3, see effect sizes in Fig. S6). When dismantling the experiment on day 36, the root compartments were inspected thoroughly. In two individual cases, a root breached the neighboring compartment; one Control sapling root was found in the Donor compartment and *vice versa*. Importantly, corresponding to these breaches, two outliers were found in the data in two Control and Donor roots. The Control that breached the Donor compartment was found to be a single outlier -9‰, and the Donor that breached the Control -12‰. Despite the unintended breach, the actual transfer that was observed reinforces that carbon transfer occurred between the trees. In order to employ a balanced statistical design, the two outlier values (out of n=326) were removed and an average of the individual sapling results the day before and after were used. The Control saplings, which were adjacent to the labeling apparatus, exhibited, across all tissues and sampling days, $\delta^{13}C$ values within natural variation and equivalent to Unlabeled Control treatment, saplings that were separated completely from the labeling apparatus (Fig. S7). As root sampling is a destructive measurement that disturbs the soil and mycelium hyphae, we minimized this disturbance by measuring the ratio between ^{13}C and ^{12}C in the gaseous phase of the soil compartment (Fig. S8). The three soil compartment denote each of the three treatments, and were measured separately. An increase in the ^{13}C in the soil compartments peaked at the 4^{th} day (18.2 ± 8.7%) for Donors and day 5 (2.66 ±1.30%) for Recipients, which afterward declined to values similar to unlabeled Control treatment. A linear regression equation was established comparing these respiration proxy values for days where elevated ^{13}C was observed between Donor and Recipient compartments (days 3-7, $R^2 = 0.64$, $F_{(1,80)} = 147.5$, $p < 0.001$; Fig. S9). Additional details are discussed in the Supplementary Information.

Mycorrhizae amplicon sequence variants were enriched in ^{13}C and colonized both donor and recipient trees

The most abundant species within the ITS2 amplicons of the tree roots were EMF (Fig. 3), reaching 98% of the reads in Donor trees and 90% in the Recipients. *Pustularia* was the most abundant genus (49% in Donors and 26% in Recipients), and in both libraries, The EMF genera *Tomentella*, *Geopora, Suillus*, *Terfezia,* and *Helvella* appeared in the top ten. *Sphaerosporella* and *Tuber* were notably more common in the Recipient than Donor trees and on *Quercus* than *Pinus* roots. After fractionation and sequencing, we compared the relative abundance results of the unlabeled gradient (day 0) and the labeled gradient (day 9) for each sapling (n=8, four Donors and their four matching Recipients) across all the ASVs (Fig. 4). MW-HR-SIP analysis was performed by defining four density windows for each ASV. MW-HR-SIP compared the normalized abundance of each ASV between the labeled (day 9) and unlabeled (day 0) SIP-gradient of each individual tree, in each

density window. The MW-HR-SIP analysis generated 125 Donors' and 233 Recipients' significantly differential abundant ASVs. However, despite the significant log fold change found, many of these ASVs had higher relative abundance only in a single SIP fraction, which we assume to be of stochastic origin and to have no biological meaning. In other cases, significant ASVs were detected as such simply because they were all but absent in the control gradients. Hence, these ASVs were ignored. Similar results were obtained after using a prevalence filter.

To validate our results, further analysis was performed using a different statistical method, the Corncob package. Corncob is a beta-binomial regression model for microbial taxon abundances, which compares an ASV relative abundance with associated covariants of interest. Corncob analysis generated similar significant ASV as MW-HR-SIP with slight variations. The list generated by Corncob of 158 and 168 ASVs for Donor and Recipient trees, respectively, was screened manually to remove false positives, i.e., ASVs that did not show the expected peak shift from unlabeled 'light' fractions to labelled 'heavy' fractions following labeling. The proportion of false positives was 42% and 56% among donors and recipients, respectively. We note, however, that most of them were either unidentified ASVs, saprophytic, or pathogenic fungal species, and not the dominant EMF species in our system. *Tomentella ellisii* was identified with labeled carbon in the Donors and Recipients of both the pine-pine and pine-oak pairs (Fig. 4b). Among pines, *Pustularia* spp., *Terfezia pini*, and *Tuber oligospermum* were also identified with ^{13}C. Additional species had labeled carbon either at Recipient or Donor sides (Fig. 4b). We used an additional analysis employing a UPLC-MS/MS protocol on the same fractionated samples of the donor library that were sequenced to ensure the incorporation of ^{13}C atoms within the DNA of the sequenced organisms. In this analysis, each nucleobase (Adenine, Guanine, Cytosine, and Thymine) was examined separately (nucleobase, as illustrated in Figs. S10, S11). An enrichment of +2, +3, and +4 ^{13}C atoms was found only in post-labeling samples (Table S4). Also, a more significant concentration of all the enrichment atoms was found in the heavier fractions. Further details are provided in the SI.

Discussion

In the present research, we demonstrated an EMF-mediated C transfer between tree saplings, irrespective of phylogenetic relatedness. We used natural forest soil as the inoculum, allowing the formation of diverse CMNs, while a mesh barrier ruled out a direct root-root transfer. The main EMF agent transferring carbon across these CMNs was *Tomentella ellisii,* the mycorrhizal partner of both

pine and oak. Six out of eight tree-pairs and all pair combinations demonstrated transfer of ^{13}C to some extent, indicating that the transfer is not strictly dictated by phylogenetic relatedness.

Leaf (Fig. S4), stem (Fig. S5), and root (Fig. 2) tissues of the Control treatment did not contain ^{13}C above natural variation, while all the tissues of the Donor trees displayed an increased $\delta^{13}C$ signature, a few folds above natural variation. In the Recipient trees, the roots were labeled above natural variation (Fig. 2), and the stem tissues were slightly labeled (Fig. S5, Fig. S6), suggesting that the transferred carbon was further distributed in the recipient plant and that the label was not restricted to the EMF mantle that surrounds the root tips, which was one of the main arguments against the idea of plant-plant C transfer (Robinson & Fitter 1999). In contrast, the recipient leaves showed no labeling at all (Fig. S4). These results lead us to conclude that ^{13}C is transferred from the roots of the Donor tree to the roots of the Recipient tree, and a small portion of ^{13}C moved against the source-sink gradient to the Recipient stem, as previously shown, albeit without temporal dynamics [32]. Even if some imported C compounds made their way up the plant and into the canopy, they were probably immensely diluted by fresh leaf assimilates, preventing their detection in leaves.

Similar to a review summarizing 47 pulse-labeling studies [26], we found a four-day lag of peak $^{13}CO_2$ efflux from the soil for pine and oak. In another review [51] focusing on ^{13}C tree labeling, 2.85 days were reported, depending on tree height and phloem structure (the average lag between labeling and efflux from soil was 3.9 ± 0.66 days for gymnosperms, 1.94 ± 0.51 days for angiosperms) placing our results in that range. Labeling done on 2.5-m tall beech trees in field conditions found equivalent temporal ^{13}C dynamics in mycorrhizal roots [52]. Similar ^{13}C labeling done on single *Quercus calliprinos* and *Pinus halepensis* saplings in our lab found similar C allocation dynamics, i.e., peak at roots three days post-labeling [43]. The variable that best explained the ^{13}C transfer between trees in our system was the amount of ^{13}C found in the whole root system of the Donor tree (Fig. S12). We found no evidence for tree species preference within the CMNs, i.e., carbon moved across species combinations irrespective of the Donor's or Recipient's identity. Earlier work found C transfer between phylogenetically distant tree species, *Pseudotsuga menziesii* and *Betula papyrifera*, primarily through EMF hyphal pathway and dictated by source-sink relationship[31]. Others showed that closely related sibling pairs exhibited more significant ^{13}C transfer compared with non-sibling pairs[34]. Our results, demonstrating carbon transfer between genetically distant trees, lend further support to the findings of Klein et al. [32] and Rog et al. [33], which demonstrated that the bidirectional transfer occurs between taxonomically distant tree taxa and that the transfer seems to be dictated by EMF that are forming CMNs between mature trees growing in a natural forest.

The pulse labeling coupled with repeated sampling strategy of tissue and respiration allowed us to trace how the ^{13}C was distributed through the Donor tree belowground and onto the Recipient tree. Combining the sequencing and DNA-SIP results, we can create a novel taxonomic list of the main EMF genera involved in C transfer among neighboring trees, pinpointing the exact taxa involved. The EMF genera *Pustularia, Terfezia, Tomentella, Tuber, Sphaerosporella, Geopora,* and *Suillus* have been found to directly receive ^{13}C from the pine Donor saplings and integrate the ^{13}C into their DNA. Separate sequencing of the paired Recipients found *Pustularia, Terfezia, Tomentella,* and *Tuber* enriched ^{13}C-DNA. *Terfezia, Tomentella,* and *Tuber* have been shown to have symbiotic interactions with both pine and oak trees [53–55]. While the host identity of *Pustularia* is unconfirmed, its function as EMF was demonstrated [56,57]. *Tomentella* was found to have ^{13}C enriched DNA in the pine Donor-oak Recipient pair (Fig. 4) and hence is considered the candidate for the formation of CMNs between these distantly related trees. *Terfezia, Tomentella,* and *Tuber* were found to have ^{13}C enriched DNA in the pine-Donor pine-Recipient pair and are therefore candidates for forming CMNs between the pines. Intriguingly, two different *Tuber* EMF species were found in pine and oak trees with ^{13}C enriched DNA, raising the question of whether the C moved across different EMF species forming CMNs (pine → *Tuber oligospermum* → *Tuber X* → oak). However, other pathways can explain these results, such as *Tuber* receiving C from the Recipient tree (tree→fungi→tree→ fungi) or absorbing it through root exudates dispersed in the soil. However, validating such mechanisms requires further observations which are beyond the scope of the current study.

Why were *Pustularia, Terfezia, Tomentella,* and *Tuber* species found to transfer C, while other EMF species that were present did not? The DNA-SIP allows us to differentiate between fungal species that were present and metabolically active, and those that came up solely in amplicon sequencing, which only identifies presence or absence. Given the natural soil inoculum that was used and that saplings were well irrigated, a fungal community proliferated, similar in its composition to that of the natural forest (Rog et al. unpublished). In turn, extra-radical mycelium was formed, resulting in ASV sequences that do not necessarily indicate function. Exploring EMF divergences such as different exploration types [58], evolutionary ecology and phylogenetic affinities [59,60], and generalist vs. specialist strategies [61], we speculate that in our system the generalist, short exploration type fungi dominated and connected dissimilar hosts. Interestingly, the Pezizales order, which was dominant in our findings, originated 150 Ma ago, around the anticipated evolution of EMF in plants. Various *Peziza* genera form a biotrophic relationship with facultative saprophytic lifestyles are common in arid and semiarid regions, and proliferate in post-fire environments which frequently occur in the

Mediterranean. The same EMF species that transfer C in our system inhabited mature trees' roots in the natural forest ecosystem which the soil was taken from (Rog et al. unpublished), including *Terfezia pini*, *Tomentella ellisii*, *Suillus collinitus*, *Tuber melosporum*, and *Tuber oligospermum.* However, these EMF species in the forest did not overlap between the mature pine and oak trees (albeit *Inocybe multifolia* and *Tricholoma terreum* did so). We presume this is due to 1. Saplings possibly being more opportunistic, forming symbiotic interactions with a broader range of symbionts to establish fitness, whereas mature trees favor more specific interactions. 2. Our experimental system might have favored short or contact EMF species interactions.

The SIP analysis was performed on root tissues nine days after the labeling, matching the peak of ^{13}C in Recipient roots. This period is long enough for carbon to be transported to root tips [62] and be assimilated into microorganisms in the rhizosphere [63,64], yet short enough so that the ^{13}C does not substantially leak into saprophytic communities. Long incubation times bear the risk of labeling community members that do not perform the metabolic activity in question: As organisms are linked through trophic interactions, labeled C will eventually spread among multiple trophic levels (cross-feeding). In addition, during sample preparation, we thoroughly washed the roots and only sampled tips that had ectomycorrhizal structures (i.e., mantle, Hartig-net;). The sampling strategy and timing of the SIP at the ninth-day post-labeling helped us avoid a common bias of DNA-SIP, namely, cross-feeding. This is further supported by the lower abundance of saprophytic sequences, compared to EMF, in all our samples (Fig. 3). Still, we cannot completely rule out the option of C transfer through soil (see below). The additional UPLC-MS/MS analysis performed here [65] is an independent analysis of the ^{13}C-DNA-SIP. The results validated that enrichment levels of +2, +3, and +4 ^{13}C atoms were found only in post-labeling gradients (Fig. S10, S11). Furthermore, the denser fractions, where the ^{13}C-DNA was expected to drift to after ultracentrifugation, had a larger quantity of enrichment levels than the low-density fractions, where ^{12}C-DNA was found. These results affirm that the DNA-SIP was performed successfully and that the potential bias of DNA-SIP caused by relative GC content of the DNA [66] did not lead to a misinterpretation of the data.

While most of the studies in the field have been dedicated to studying C transfer through CMNs, there are other plausible explanations for how C is being transferred among trees. Other microorganisms might have been involved in the process of ^{13}C transfer, and, in addition, C might move by passive diffusion. These mechanisms are non-mutually exclusive and might co-occur at different spatial and temporal scales. While the current design cannot rule out these other mechanisms, we can inquire about the probability of their role in the temporal timeline ^{13}C appeared

in the system. $^{13}CO_2$ respiration appeared in the recipient compartment as early as three days post-labeling and as early as four days in roots. One possible mechanism of C transfer is direct root grafting among trees. However, this option is ruled out by most CMNs studies, including ours, by using a dense mesh-net control that prevents root to root interaction [21]. Another mechanism of C transfer involves other microorganisms such as bacteria living in the rhizosphere while feeding on root exudates [67]. As elegantly shown by Gorka *et al*., [28], EMF can receive photosynthetically derived C and further transfer it to bacteria in the soil adjacent to hyphal tips (i.e., hyphosphere). These complex interactions can occur via direct symbiosis [68] or indirectly through C turnover in the soil. For bacteria to be the main C mediators, the bacteria need to absorb ^{13}C exudates secreted by a donor root, finish its life cycle, degrade, and be absorbed by at least a few other microorganisms to bridge over the few millimeters distance between the donor and recipient roots. Bacterial turnover in the soil is a complex interaction involving many factors [69], and separate 16S qPCR or DNA-SIP analysis must be done to understand their role. We speculate that their involvement to be neglectable because the temporal processes that need to occur for the bacteria to transfer C to neighboring trees do not align with the temporal timescale ^{13}C that appeared in the recipient compartment. Lastly, passive C diffusion between Donor and Recipient compartment through the soil matrix is another possible mechanism for C transfer, which requires the uptake of C from the soil by the tree roots. However, evidence for such phenomena in mature forest trees is scarce. We presume passive diffusion of C does not add a significant contribution in the timescale we found ^{13}C in the recipient compartment. Although dissolved inorganic carbon (DIC) processes are instantaneous, they depend on pH, water availability, and temperature. Water infiltration needs to be calculated to convert rates of change in DIC to a function of distance by time. We calculated 72-100 cm $year^{-1}$ i.e. 0.8-1.1 cm in four days (regression equation; Precipitation (P)= 510 mm $year^{-1}$; infiltration rate (cm $year^{-1}$) = 0.4057(P) - 107.13; $R^2 = 0.96$ with n = 4. value derived from Beit Shemesh, where the soil was taken from, Qubaja unpublished data). This calculation is adapted from Carmi et al. [70], which calculated the rate in a drier pine forest. In this study, we used similar soil and tree saplings derived from a natural system. Mixing with sand (see Methods) possibly increased the abovementioned rate, since infiltration rate in sand is maximal, and hence the opportunity for C dissolution should be lower. Therefore, it seems that passive diffusion is a few orders of magnitudes slower than when ^{13}C appeared in the recipient compartment. Moreover, all the experimental units contained the same soil mixture and were watered to the same extent, the fact that we did not observe any transfer of C in some of our mesocosms deteriorates passive C diffusion from being the main mechanism for C transfer in our system.

In the broader context of natural forest ecology, questions arise regarding the ecophysiological and ecological significance of the inter-plant C transfer through CMNs. More specifically, what could be the significance of the small amounts of C transferred from donor trees to recipient trees for the carbon balance of the latter? Despite the use of natural soil inoculum in our microcosm design, we tread lightly when wishing to interpret our results in the broader forest ecology context, considering that saplings age and size, irrigation, and the fixed distance between plants are far from representing the forest. Still, we showed that C transfer through mycorrhiza increased the $\delta^{13}C$ of recipient saplings from -26‰ to -13‰ in roots, and from -27‰ to -22‰ in the stem (Fig. 1). Using a simple two-end linear mixing model, both of these increases are explained by an import of 0.5% of root C from the donor. This value was maintained across the different species combinations in our experiment, despite the variations among them. Considering that root and stem biomass were 22 and 56 g, respectively, this imported C fraction amounts to 1.1 g and 2.8 g in roots and stem, respectively. These estimates are smaller than those calculated for a 5-year labeling in a forest, where carbon transfer accounted for 4% of tree carbon uptake [33]. Importantly, pulse labeling experiments (as described here) are useful for capturing short-term dynamics [43], yet are limited in their ability to decipher long-term carbon allocation [71]. Therefore, we assume that at the long-term, the rate of imported carbon is higher than 0.5%. Nevertheless, even small amounts of C import might serve to alleviate the EMF partnership C cost of the recipient tree at the local root level [72]. Increased fitness of these roots may play an important role in survival of saplings suffering low C supply due to growth in the shade of older trees [73]. Alternatively, if the transfer is in the form of amino acids or other nitrogen-containing compounds (as would be expected in a mycorrhizal association; [72], C is rather a by-product of nitrogen transfer and hence low in amount. These aspects are yet unresolved and are the topic of follow-up manipulation experiments.

The importance of EMF symbiosis to the balanced functioning of forest ecosystems is well established and unquestionable. However, our understanding stops at the plant-fungi relationship, as data are limited on how these connections distribute further and scale to form networks. For example, Van Der Heijden and Horton [74] elegantly raised the question of "who dictates the symbiotic interaction among plants and their fungal partners?"; is it a "socialist" relationship where both the plant and fungi have equal opportunities and nutrients are evenly distributed, or rather a "capitalist" network where the plant establishes and nourishes the networks, solely controlling the nutrient profit? The first step in shedding light on these essential questions is identifying the key players in this symbiotic relationship, which we successfully achieved in the study. Follow-up studies focus on experimental manipulations to identify the ecological significance of the C being transferred via

CMNs. By improving our knowledge of these key players' identity and ecological role, we will better comprehend the interactions shaping forest biomes.

Acknowledgments

The authors wish to thank Ido Rog (Weizmann TreeLab) for help with the labeling system; Ishai Sher (WIS) for his help with the graphic design; and Alexander Brandis (WIS) for his help with performing MSMS analysis. RA was supported by MEYS (EF16_013/0001782 - SoWa Ecosystems Research). The study was funded by the European Research Council project RHIZOCARBON, granted to TK.

Data availability statement

Sequences were submitted to the National Center for Biotechnology Information Sequence Read Archive with the accession codes: Bioproject PRJNA777920.

Conflict of interest statement

We declare no conflict of interest and that this material has not been submitted for publication elsewhere.

Author contributions

TK, SLL and RC conceived and designed the experiment. RC and SLL performed the experiment and analyzed the data under the guidance of TK. SIP procedures and analysis were guided by RA. RC wrote the paper with SLL and TK, and all authors contributed substantially to revisions.

References

1. Steidinger BS, Crowther TW, Liang J, Van Nuland ME, Werner GD, Reich PB *et al*. Climatic controls of decomposition drive the global biogeography of forest-tree symbioses. *Nature* **569**, 404–408 (2019).
2. Finlay RD. Ecological aspects of mycorrhizal symbiosis: with special emphasis on the functional diversity of interactions involving the extraradical mycelium. *J. Exp. Bot.* **59**, 1115–1126 (2008).
3. Smith SE, Read D. Nitrogen mobilization and nutrition in ectomycorrhizal plants. *Mycorrhizal Symbiosis* 321–348 (2008) doi:10.1016/b978-012370526-6.50011-8.
4. Osonubi O, Mulongoy K, Awotoye OO, Atayese MO, Okali DUU. Effects of ectomycorrhizal and vesicular-arbuscular mycorrhizal fungi on drought tolerance of four leguminous woody seedlings. *Plant Soil* **136**, 131–143 (1991).
5. Mayerhofer W, Schintlmeister A, Dietrich M, Gorka S, Wiesenbauer J, Martin V, *et al.* Ectomycorrhizal fungi induce systemic resistance against insects on a nonmycorrhizal plant in a CERK1-dependent manner. *New Phytol.* **228**, 728–740 (2020).
6. Mayerhofer W, Schintlmeister A, Dietrich M, Gorka S, Wiesenbauer J, Martin V. *et al*. Mycorrhizal networks: mechanisms, ecology and modelling. *Fungal Biol. Rev.* **26**, 39–60 (2012).
7. Molina R, Horton TR. Mycorrhiza specificity: its role in the development and function of common mycelial networks. *Mycorrhizal networks* (2015). doi:10.1007/978-94-017-7395-9_1.
8. Van der Heijden MG A, Martin FM, Selosse MA, Sanders IR. Mycorrhizal ecology and evolution: the past, the present, and the future. *New Phytol.* **205**, 1406–1423 (2015).
9. Brundrett MC. Coevolution of roots and mycorrhizas of land plants. *New Phytol.* **154**, 275–304 (2002).
10. Linkies A, Graeber K, Knight C, Leubner-Metzger G. The evolution of seeds. *New Phytol.* **186**, 817–831 (2010).
11. Nara K. Ectomycorrhizal networks and seedling establishment during early primary succession. *New Phytol.* **169**, 169–178 (2006).
12. Horton TR., Molina R, Hood K. Douglas-fir ectomycorrhizae in 40- and 400-year-old stands: mycobiont availability to late successional western hemlock. *Mycorrhiza* **15**, 393–403 (2005).
13. Teste FP, Simard SW, Durall DM, Guy RD, Jones MD, Schoonmaker AL. Access to mycorrhizal networks and roots of trees: importance for seedling survival and resource transfer. *Ecology* **90**, 2808–2822 (2009).

14. Teste FP, Simard SW. Mycorrhizal networks and distance from mature trees alter patterns of competition and facilitation in dry Douglas-fir forests. *Oecologia* **158**, 193–203 (2008).
15. Egerton-Warburton LM, Querejeta JI, Allen MF. Common mycorrhizal networks provide a potential pathway for the transfer of hydraulically lifted water between plants. *J. Exp. Bot.* **58**, 1473–1483 (2007).
16. Wallander H, Ekblad A. The Importance of ectomycorrhizal networks for nutrient retention and carbon sequestration in forest ecosystems. *Mycorrhizal Networks* **69–90** (2015) doi:10.1007/978-94-017-7395-9_3.
17. Song YY, Simard SW, Carroll A, Mohn WW, Zeng RS. Defoliation of interior Douglas-fir elicits carbon transfer and stress signalling to ponderosa pine neighbors through ectomycorrhizal networks. *Sci. Rep.* **5**, 1–9 (2015).
18. Selosse MA, Richard F, He X, Simard SW. Mycorrhizal networks: des liaisons dangereuses? *Trends Ecol. Evol.* **21**, 621–628 (2006).
19. Robinson D, Fitter A. The magnitude and control of carbon transfer between plants linked by a common mycorrhizal network. *J. Exp. Bot.* **50**, 9–13 (1999).
20. Hoeksema JD. Experimentally testing effects of mycorrhizal networks on plant-plant interactions and distinguishing among mechanisms. *Mycorrhizal Networks* **255–277** (2015) doi:10.1007/978-94-017-7395-9_9.
21. Teste FP, Karst J, Jones MD, Simard SW, Durall DM. Methods to control ectomycorrhizal colonization: effectiveness of chemical and physical barriers. *Mycorrhiza* **17**, 51–65 (2006).
22. Graves JD, Watkins NK, Fitter AH, Robinson D, Scrimgeour C. Intraspecific transfer of carbon between plants linked by a common mycorrhizal network. *Plant Soil* **192**, 153–159 (1997).
23. Wu B, Nara K, Hogetsu T. Can ^{14}C-labeled photosynthetic products move between Pinus densiflora seedlings linked by ectomycorrhizal mycelia? *New Phytol.* **149**, 137–146 (2001).
24. Bever JD, Dickie IA, Facelli E, Facelli JM, Klironomos J, Moora M. *et al*. Rooting theories of plant community ecology in microbial interactions. *Trends in ecology & evolution*. **25(8)**, 468-78 (2010).
25. Scheublin TR, Van Logtestijn RSP, Van Der Heijden MGA. Presence and identity of arbuscular mycorrhizal fungi influence competitive interactions between plant species. *J. Ecol.* **95**, 631–638 (2007).
26. Epron D, Bahn M, Derrien D, Lattanzi FA, Pumpanen J, Gessler A. *et al*. Pulse-labelling trees to study carbon allocation dynamics: A review of methods, current knowledge and future

prospects. *Tree Physiol.* **32**, 776–798 (2012).

27. Whiteside MD, Werner GD, Caldas VE, Padje A, Dupin SE, Elbers B. *et al*. Mycorrhizal fungi respond to resource inequality by moving phosphorus from rich to poor patches across networks. *Curr. Biol.* **29**, 2043-2050.e8 (2019).
28. Gorka S, Dietrich M, Mayerhofer W, Gabriel R, Wiesenbauer J, Martin V. *et al*. Rapid transfer of plant photosynthates to soil bacteria via ectomycorrhizal hyphae and its interaction with nitrogen availability. *Front. Microbiol.* **10**, 1–20 (2019).
29. Leake JR, Donnelly DP, Saunders EM, Boddy L, Read DJ. Rates and quantities of carbon flux to ectomycorrhizal mycelium following ^{14}C pulse labeling of Pinus sylvestris seedlings: effects of litter patches and interaction a wood-decomposer fungus. *Tree Physiol.* **21**, 71–82 (2001).
30. Kiers ET, Duhamel M, Beesetty Y, Mensah JA, Franken O, Verbruggen E, *et al*. Reciprocal rewards stabilize cooperation in the mycorrhizal symbiosis. *Science.* **333**, 880–882 (2011).
31. Simard SW, Perry DA, Jones MD, Myrold DD, Durall DM, Molina R. Net transfer of carbon between ectomycorrhizal tree species in the field. *Nature* **388**, 579–582 (1997).
32. Klein T, Siegwolf RTW, Körner C. Belowground carbon trade among tall trees in a temperate forest. *Science*. **1500**, 15–18 (2016).
33. Rog I, Rosenstock NP, Körner C, Klein T. Share the wealth: Trees with greater ectomycorrhizal species overlap share more carbon. *Mol. Ecol.* **29**, 2321–2333 (2020).
34. Pickles BJ, Wilhelm R, Asay AK, Hahn AS, Simard SW, Mohn WW.Transfer of ^{13}C between paired Douglas-fir seedlings reveals plant kinship effects and uptake of exudates by ectomycorrhizas. *New Phytol.* **214**, 400–411 (2017).
35. Lu Y, Conrad R. In situ stable isotope probing of methanogenic Archaea in the rice rhizosphere. *Science*. **309**, 1088–1090 (2005).
36. Haichar Z, Heulin T, Guyonnet JP, Achouak W. Science direct stable isotope probing of carbon flow in the plant holobiont. *Curr. Opin. Biotechnol.* **41**, 9–13 (2016).
37. Sietiö OM, Tuomivirta T, Santalahti M, Kiheri H, Timonen S, Sun H. *et al.* Ericoid plant species and Pinus sylvestris shape fungal communities in their roots and surrounding soil. *New Phytol.* **218**, 738–751 (2018).
38. Sapes G, Demaree P, Lekberg Y, Sala A. Plant carbohydrate depletion impairs water relations and spreads via ectomycorrhizal networks. *New Phytol.* **229**, 3172–3183 (2021).
39. Sheffer E. A review of the development of Mediterranean pine-oak ecosystems after land abandonment and afforestation: are they novel ecosystems? *Ann. For. Sci.* **69**, 429–443 (2012).

40. Ajbilou R, Marañón T, Arroyo J. Ecological and biogeographical analyses of Mediterranean forests of northern Morocco. *Acta Oecologica* **29**, 104–113 (2006).
41. Loudermilk E, Hiers J, Pokswinski S, O'Brien JJ, Barnett A, Mitchell RJ. The path back: Oaks (Quercus spp.) facilitate longleaf pine (Pinus palustris) seedling establishment in xeric sites. *Ecosphere* **7**, 1–14 (2016).
42. Hynes MM, Smith ME, Zasoski RJ, Bledsoe, CS. A molecular survey of ectomycorrhizal hyphae in a California Quercus-Pinus woodland. *Mycorrhiza* **20**, 265–274 (2010).
43. Rog I, Jakoby G, Klein T. Forest ecology and management carbon allocation dynamics in conifers and broadleaved tree species revealed by pulse labeling and mass balance. *For. Ecol. Manage.* **493**, 119258 (2021).
44. Jia Z, Cao W, Herna M. DNA-Based stable isotope probing. *Springer* **2046**, 17–29 (2019).
45. Neufeld JD, Vohra J, Dumont MG, Lueders T, Manefield M, Friedrich MW. *et al*. DNA stable-isotope probing. *Nat. Protoc.* **2**, 860–866 (2007).
46. Taylor DL, Walters WA, Lennon NJ, Bochicchio J, Krohn A, Caporaso JG. *et al*. Accurate estimation of fungal diversity and abundance through improved lineage-specific primers optimized for Illumina amplicon sequencing. *Appl. Environ. Microbiol.* **82**, 7217–7226 (2016).
47. Blecher-Gonen R, Barnett-Itzhaki Z, Jaitin D, Amann-Zalcenstein D, Lara-Astiaso D, Amit I. High-throughput chromatin immunoprecipitation for genome-wide mapping of in vivo protein-DNA interactions and epigenomic states. *Nat. Protoc.* **8**, 539–554 (2013).
48. Callahan BJ, McMurdie PJ, Rosen MJ, Han AW, Johnson AJA, Holmes SP. DADA2: High-resolution sample inference from Illumina amplicon data. *Nat. Methods* **13**, 581–583 (2016).
49. Buckley DH, Barnett SE, Youngblut ND. Data analysis for DNA stable isotope probing experiments using multiple window high-resolution SIP Chapter 9. *Springer* **2046**, 44–45 (2019).
50. Martin BD, Witten D, Willis AD. Modeling microbial abundances and dysbiosis with beta-binomial regression. *Ann. Appl. Stat.* **14**, 94–115 (2020).
51. Kuzyakov Y, Gavrichkova O. time lag between photosynthesis and carbon dioxide efflux from soil: a review of mechanisms and controls. *Glob. Chang. Biol.* **16**, 3386–3406 (2010).
52. Hagedorn F, Joseph J, Peter M, Luster J, Pritsch K, Geppert U. *et al*. Recovery of trees from drought depends on belowground sink control. *Nat. Plants* **2**, (2016).
53. Moreno-Arroyo B, Infante F, Pulido E, Gómez J. The biogeography and taxonomy of Tuber oligospermum (Tul. and C. Tul.) Trappe (Ascomycota). *Cryptogam. Mycol.* **21**, 147–152 (2000).

54. Buscardo E, Rodríguez-Echeverría S, Martín MP, De Angelis P, Pereira JS, Freitas H. Impact of wildfire return interval on the ectomycorrhizal resistant propagules communities of a Mediterranean open forest. *Fungal Biol.* **114**, 628–636 (2010).
55. Louro R, Santos-Silva C, Nobre T. What is in a name? Terfezia classification revisited. *Fungal Biol.* **123**, 267–273 (2019).
56. Tedersoo L, Arnold AE, Hansen K. Novel aspects in the life cycle and biotrophic interactions in Pezizomycetes (Ascomycota, Fungi). *Mol. Ecol.* **22**, 1488–1493 (2013).
57. Tedersoo L, Smith ME. Lineages of ectomycorrhizal fungi revisited: Foraging strategies and novel lineages revealed by sequences from belowground. *Fungal Biol. Rev.* **27**, 83–99 (2013).
58. Agerer R. Fungal relationships and structural identity of their ectomycorrhizae. *Mycol. Prog.* **5**, 67–107 (2006).
59. Tedersoo L, May TW, Smith ME. Ectomycorrhizal lifestyle in fungi: global diversity, distribution, and evolution of phylogenetic lineages. *Mycorrhiza* **20**, 217–263 (2010).
60. Miyauchi S, Kiss E, Kuo A, Drula E, Kohler A, Sánchez-García M, Martin FM. *et al*. Large-scale genome sequencing of mycorrhizal fungi provides insights into the early evolution of symbiotic traits. *Nat. Commun.* **11**, 1–17 (2020).
61. Bruns TD, Bidartondo MI, Taylor DL. Host specificity in ectomycorrhizal communities: what do the exceptions tell us? *Integr. Comp. Biol.* **42**, 352–359 (2002).
62. Pumpanen JS, Heinonsalo J, Rasilo T, Hurme KR, Ilvesniemi H. Carbon balance and allocation of assimilated CO_2 in Scots pine, Norway spruce, and Silver birch seedlings determined with gas exchange measurements and ^{14}C pulse labelling. *Trees - Struct. Funct.* **23**, 611–621 (2009).
63. Heinonsalo J, Pumpanen J, Rasilo T, Hurme KR. & Ilvesniemi, H. Carbon partitioning in ectomycorrhizal Scots pine seedlings. *Soil Biol. Biochem.* **42**, 1614–1623 (2010).
64. Wallander H, Göransson H, Rosengren U. Production, standing biomass and natural abundance of ^{15}N and ^{13}C in ectomycorrhizal mycelia collected at different soil depths in two forest types. *Oecologia* **139**, 89–97 (2004).
65. Wilhelm R, Szeitz A, Klassen TL, Mohn WW. Sensitive, efficient quantitation of ^{13}C-enriched nucleic acids via ultrahigh-performance liquid chromatography-tandem mass spectrometry for applications in stable isotope probing. *Appl Environ Microbiol*. **80**, 7206-7211 (2014). doi:10.1128/AEM.02223-14
66. Schildkraut CL, Marmur J, Doty P. Determination of the base composition of deoxyribonucleic acid from its buoyant density in CsCl. *J. Mol. Biol.* **4**, 430–443 (1962).
67. Jakoby G, Rog I, Megidish S, Klein T. Enhanced root exudation of mature broadleaf and

conifer trees in a Mediterranean forest during the dry season. *Tree Physiol.* **40**, 1595–1605 (2020).

68. Meier IC, Pritchard SG, Brzostek ER, Mccormack ML, Phillips RP. The rhizosphere and hyphosphere differ in their impacts on carbon and nitrogen cycling in forests exposed to elevated CO_2. *New Phytol.* **205**, 1164–1174 (2015).
69. Ranjard L, Dequiedt S, Prévost-Bouré NC, Thioulouse J, Saby NPA, Lelievre M. *et al*. Turnover of soil bacterial diversity driven by wide-scale environmental heterogeneity. *Nat. Commun.* **4**, (2013).
70. Carmi I, Yakir D, Yechieli Y, Kronfield J, Stiller M. Variations in the isotopic composition of dissolved inorganic carbon in the unsaturated zone of a semi-arid region. *Radiocarbon*, **57** (3), 397-406 (2015).
71. Klein T, Hoch G. Tree carbon allocation dynamics determined using a carbon mass balance approach. *New Phytol.* **205**, 147–159 (2015).
72. Mayerhofer W, Schintlmeister A, Dietrich M, Gorka S, Wiesenbauer J, Martin V. *et al*. Recently photoassimilated carbon and fungus-delivered nitrogen are spatially correlated in the ectomycorrhizal tissue of Fagus sylvatica. *New Phytol.* **232**, 2457-2474 (2021) doi:10.1111/nph.17591.
73. Fraser EC, Lieffers VJ, Landhäusser SM. Carbohydrate transfer through root grafts to support shaded trees. *Tree Physiol.* **26**, 1019–1023 (2006).
74. Van Der Heijden MGA, Horton TR. Socialism in soil? the importance of mycorrhizal fungal networks for facilitation in natural ecosystems. *J. Ecol.* **97**, 1139–1150 (2009).
75. Wu B, Nara K, Hogetsu T. Can ^{14}C-labelled photosynthetic products move between *Pinus densiflora* seedlings linked by ectomycorrhizal mycelia? *New Phytologist*, **149**, 137–146 (2001).

Tables and Figures

Table 1. The statistical model summarizes the $\delta^{13}C$ values in the root tissues (ANOVA on repeated samples). Significance codes: <0.001 '***' 0.001 '**' 0.01 '*' 0.05. Df denotes degrees of freedom, Sq denotes square root.

Error: Pot ID	Df	Sum Sq	Mean Sq	F value	Pr(>F)
Pairs	3	12073370	4024457	0.71	0.59
Residuals	4	22689574	5672394		
Error: Within	Df	Sum Sq	Mean Sq	F value	Pr(>F)
Days	10	23062398	2306240	3.87	0.0001 ***
Treatment	2	293387304	146693652	246.29	< 2e-16 ***
Pairs:Days	30	7193976	239799	0.40	0.99
Pairs:Treatment	6	23684010	3947335	6.63	4.02e-06 ***
Days:Treatment	20	45709518	2285476	3.84	1.60e-06 ***
Pairs:Days:Treatment	60	14337623	238960	0.40	0.99
Residuals	128	76238157	595611		

Captions to Figures

Figure 1. Evidence for ^{13}C transfer in the *Quercus – Pinus – Quercus* combination (n=2). The orange arrow denotes ^{13}C transfer as it passed across kingdoms, from tree to fungi and on to another tree, facilitated through the EMF specie *Tomentella ellisii*. White arrows denote ^{13}C allocation within the tree tissues. Values are averages±SE of samples taken along time-points: stem (n=3), leaves (n=11) and roots (n=10).

Figure 2. Root $\delta^{13}C$ of three treatments: Donor, Recipient, and Control (top to bottom). Triangles and asterisks denote different biological replicates (n=2) of each pair combination. Vertical panels represent pair combinations (Donor → Recipient). A grey area marks the $\delta^{13}C$ natural variation of -24‰ and below.

Figure 3. (a) Rank abundance curve of the relative abundances of fungal genera based on ITS2 amplicon-sequencing. The results are derived from four pine donors and their recipient pairs. The remaining oak donors and their corresponding pairs were not sequenced. (b) Heat map summarizing the relative abundance of the top seven EMF genera in each of the eight trees that were sequenced. Pairs' color annotation (top boxes) denotes the donor and recipient tree pairs (Donor → Recipient). Euclidean clustering denotes how the trees clustered together.

Figure 4. (a) ^{13}C-DNA-SIP results depicting *Tomentella* ^{13}C-enriched ASV buoyant density of the fractions compared to the relative abundance; right graph represents DNA from the oak recipient and the left graph from the pine donor*;* both display an increase of relative abundance in 'heavy' (^{13}C) fractions. Pre- and post-labeling are represented by days 0 and 9, respectively. Green and yellow areas highlight the fractions where ^{13}C- and ^{12}C-DNA is expected to be found. (b) Venn diagrams depicting the number and identity of shared ^{13}C-enriched ASVs of the four pair combinations (donors in grey; recipients in yellow). Total ^{12}C- ASV are shown after prevalence filter and quantitative filters.

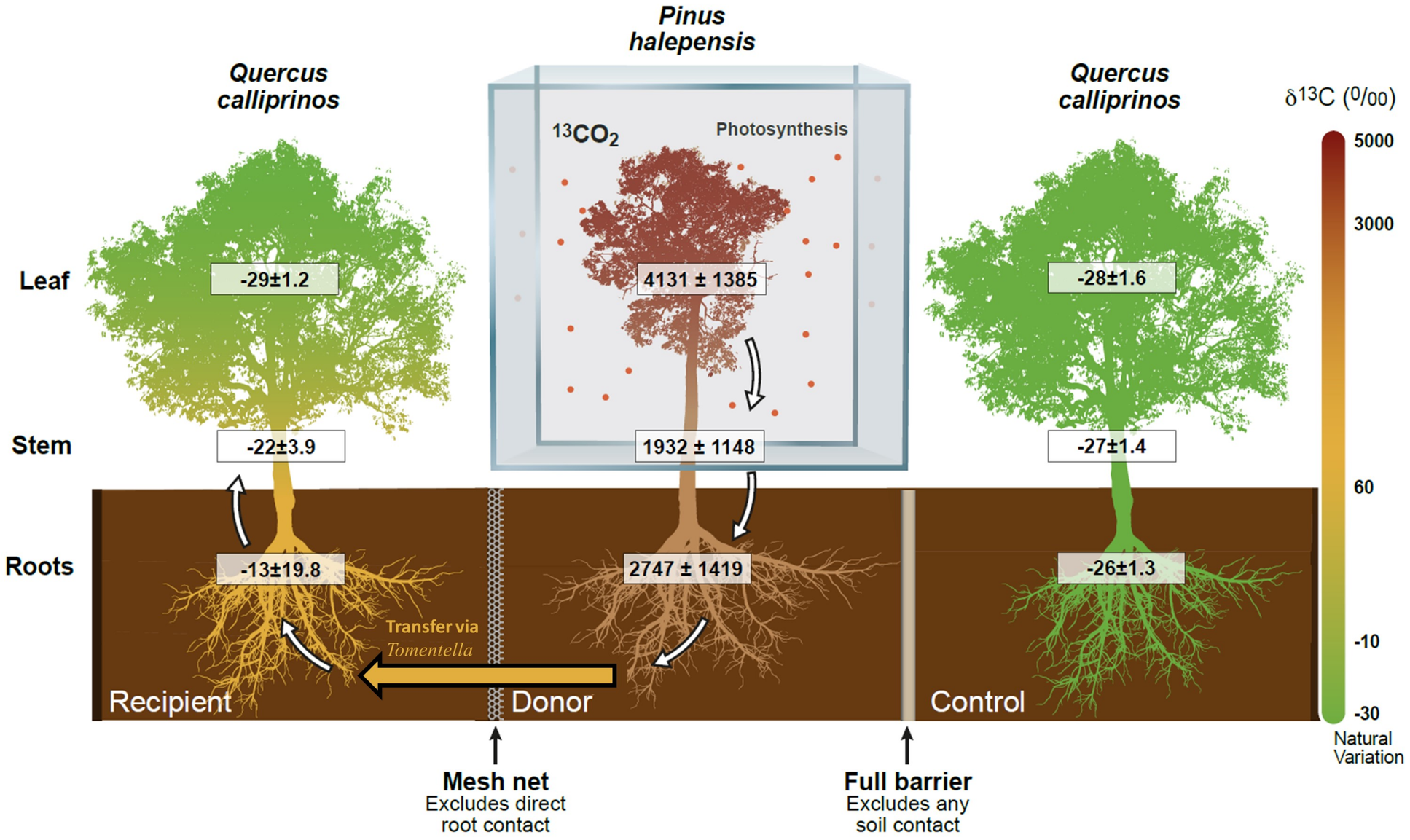
Pinus halepensis
Quercus calliprinos
Quercus calliprinos
δ13C (0/00)
13CO2
Photosynthesis
Leaf
Stem
Roots
-29±1.2
-22±3.9
-13±19.8
4131 ± 1385
1932 ± 1148
2747 ± 1419
-28±1.6
-27±1.4
-26±1.3
Transfer via
Tomentella
Recipient
Donor
Control
5000
3000
60
-10
-30
Natural Variation
Mesh net
Excludes direct root contact
Full barrier
Excludes any soil contact

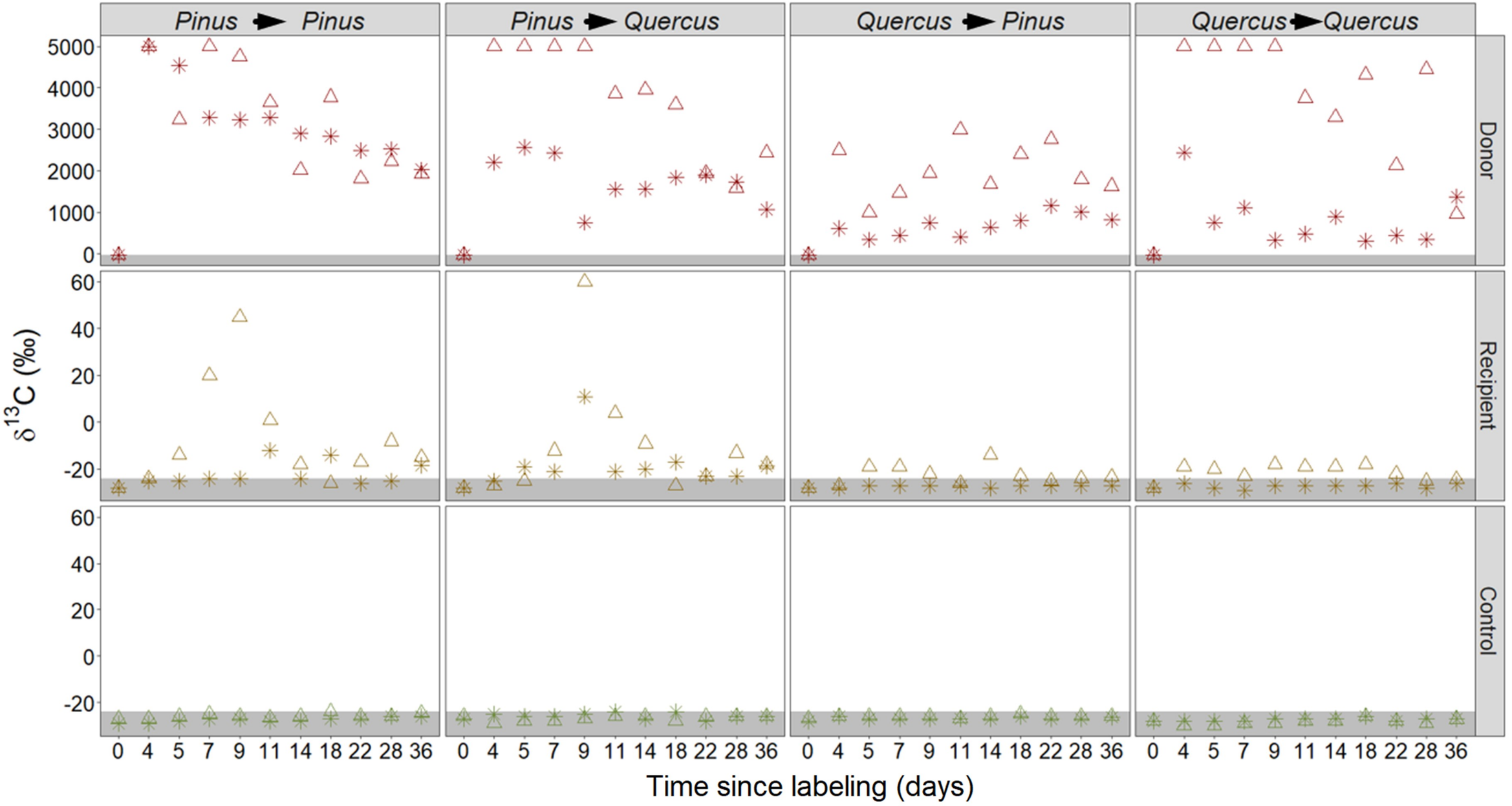
Pinus → Pinus
Pinus → Quercus
Quercus → Pinus
Quercus → Quercus
Donor
Recipient
Control
δ13C (‰)
5000
4000
3000
2000
1000
0
60
40
20
0
-20
0 4 5 7 9 11 14 18 22 28 36
Time since labeling (days)

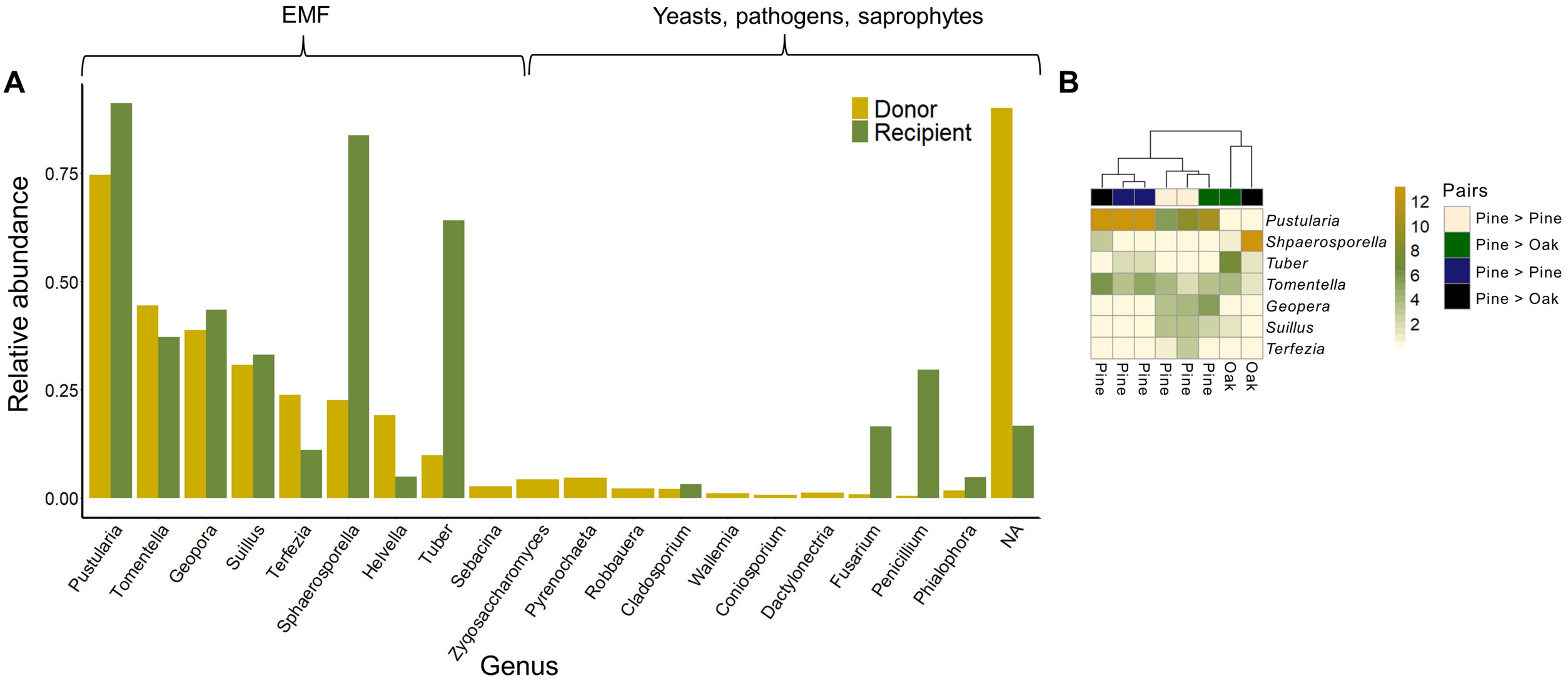
EMF
Yeasts, pathogens, saprophytes
A
B
Donor
Recipient
Relative abundance
0.00
0.25
0.50
0.75
Pustularia
Tomentella
Geopora
Suillus
Terfezia
Sphaerosporella
Helvella
Tuber
Sebacina
Zygosaccharomyces
Pyrenochaeta
Robbauera
Cladosporium
Wallemia
Coniosporium
Dactylonectria
Fusarium
Penicillium
Phialophora
NA
Genus
Pustularia
Shpaerosporella
Tuber
Tomentella
Geopera
Suillus
Terfezia
Pine
Pine
Pine
Pine
Pine
Pine
Oak
Oak
12
10
8
6
4
2
Pairs
Pine > Pine
Pine > Oak
Pine > Pine
Pine > Oak

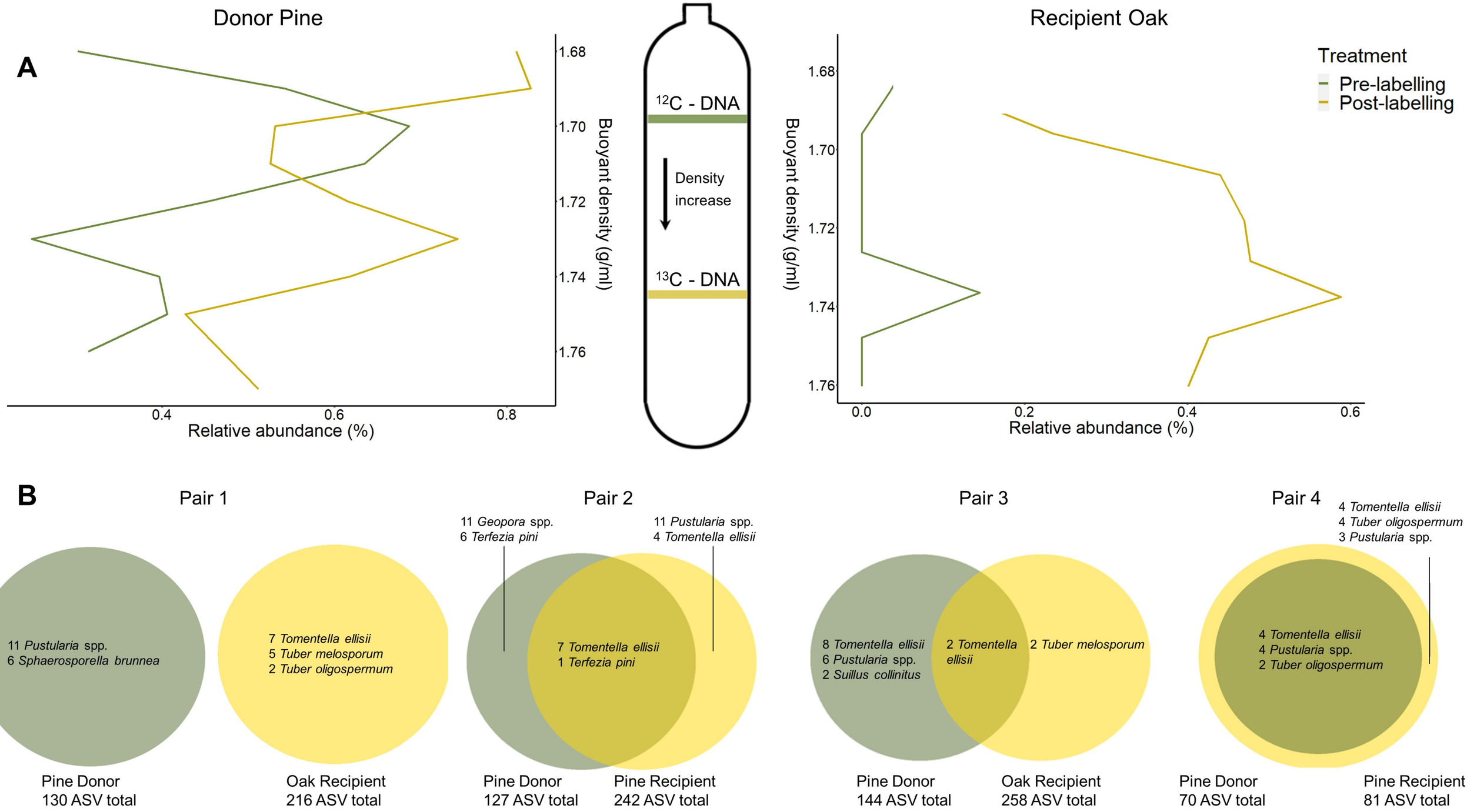
A
Donor Pine
Recipient Oak
Buoyant density (g/ml)
1.68
1.70
1.72
1.74
1.76
0.4
0.6
0.8
0.0
0.2
Relative abundance (%)
12C - DNA
13C - DNA
Density
increase
Treatment
Pre-labelling
Post-labelling
B
Pair 1
11 Pustularia spp.
6 Sphaerosporella brunnea
7 Tomentella ellisii
5 Tuber melosporum
2 Tuber oligospermum
Pine Donor
130 ASV total
Oak Recipient
216 ASV total
Pair 2
11 Geopora spp.
6 Terfezia pini
11 Pustularia spp.
4 Tomentella ellisii
7 Tomentella ellisii
1 Terfezia pini
Pine Donor
127 ASV total
Pine Recipient
242 ASV total
Pair 3
8 Tomentella ellisii
6 Pustularia spp.
2 Suillus collinitus
2 Tomentella ellisii
2 Tuber melosporum
Pine Donor
144 ASV total
Oak Recipient
258 ASV total
Pair 4
4 Tomentella ellisii
4 Tuber oligospermum
3 Pustularia spp.
4 Tomentella ellisii
4 Pustularia spp.
2 Tuber oligospermum
Pine Donor
70 ASV total
Pine Recipient
81 ASV total